# Synthesis and characterization of amine-functionalized microgel particles and their subsequent assembly into colloidal molecule-like clusters by droplet-based microfluidics

B.Sc. Thesis, 15 hp

*Author:*
Emil Gustafsson

*Supervisors:*
Prof. Peter Schurtenberger
Linda Månsson
Feifei Peng

*Examiner:*
Prof. Lennart Piculell

August 24, 2015

*"No agression, only aggregation."*

- Ellen, Maria and Maria.

# Populärvetenskaplig sammanfattning

Kolloider är partiklar i storleksordningen nm till $\mu$m. De är viktiga i biologiska system, där exempelvis proteiner är en typ av kolloid. Att studera kolloider ger oss därför insikt i hur till exempel proteiner byggs upp och interagerar. I detta fall försökte vi tillverka kolloidala molekyler, alltså kolloider som interagerar med varandra genom ett specifikt antal bindningar i väl definierade positioner och riktningar. För att skapa kolloidala molekyler användes mikrogeler som sammansattes till kluster, där antalet bindningar och dess riktning bestäms av antalet mikrogeler och dess position. Mikrogeler är kolloidala partiklar med temperaturberoende egenskaper. Under en viss kritisk temperatur är mikrogelerna stora och vattenälskande och på grund av detta absorberar de vatten. Över den kritiska temperaturen skyr mikrogelerna vatten och krymper ihop. Ändring i temperatur påverkar inte enbart mikrogelernas storlek utan också hur de interagerar med varandra; över den kritiska temperaturen tycker mikrogelerna om att interagera med varandra. Kolloidala molekyler som tillverkas av mikrogeler får mikrogelernas temperaturberoende egenskaper och således kan klustrens egenskaper också styras genom temperaturen.

För att kunna skapa kluster av mikrogeler behöver mikrogelerna tillverkas så att möjlighet finns att binda ihop dem med varandra. Mikrogelerna tillverkades därför med amingrupper som fungerar som brofästen. Glutaraldehyd fäster vid amingrupperna och kunde då användas som bro mellan två mikrogeler. För att få mikrogelerna att komma tillräckligt nära varandra, både för att bilda kluster och för att bygga broar mellan dem, så bildade vi vattendroppar innehållande både mikrogeler och glutaraldehyd. Mikrogelerna tvingades närmare varandra i vattendropparna genom att dropparna krymptes. Klustren som bildas antar olika form beroende på hur många mikrogeler som deltar.

Fyra olika mikrogeler tillverkades från två olika temperaturkänsliga polymerer, det vill säga långa kedjor av upprepade mindre enheter, och färgades med fluorescerande molekyler. Vi har kunnat visa att mikrogelerna kan bindas ihop genom att låta dem bilda tvärbundna nätverk, geler, från lösningar. Kluster av mikrogeler har inte kunnat isoleras efter droppkrympning, men detta är något som vi hoppas kunna göra i framtiden.

# Abstract

The ability of thermoresponsive, amine-functionalized microgel particles to take part in microgel-microgel inter-cross-linking has previously been reported in the literature, in connection to applications such as for example the formation of stimuli-responsive colloidal gels and colloidosomes.[1] This thesis deals with the synthesis of such thermoresponsive, cross-linkable microgels and their subsequent assembly into clusters using droplet-based microfluidics, with the goal of forming responsive colloidal molecules with well-defined valency. Such colloidal molecules can be used as model systems to study controlled self-assembly processes.

In this project, monodisperse amine-functionalized poly(*N*-isopropylacrylamide) (PNIPAM) and poly(*N*-isopropylmethacrylamide) (PNIPMAM) microgels, cross-linkable with glutaraldehyde, were synthesized. In total, four microgel systems were produced and the microgels were subsequently characterized by dynamic and static light scattering (DLS and SLS), confocal laser scanning microscopy (CLSM) and electrophoretic mobility. The microgels were shown to exhibit termoresponsive behavior with respect to size, charge density and interaction potential. In the presence of glutaraldehyde, dense microgel suspensions were converted to macrogels through microgel-microgel cross-linking. Upon heating the macrogels to above the microgels' volume phase transition temperature (VPTT), they contracted, thus showing that the thermoresponsive behavior of the microgels was conferred to the macrogels. The obtained microgel systems were then used in droplet-based microfluidics to generate colloidal molecule-like clusters. However, the presence of clusters could not be confirmed, likely due to problems with extraction.

[1] a) G. Huang, J. Gao, Z. Hu, J. V. St. John, B. C. Ponder and D. Moro. Controlled Drug Release from Hydrogel Nanoparticle Networks. *J. Control. Release*, 94:303-311, 2004. b) G. Huang and Z. Hu. Phase Behavior and Stabilization of Microgel Arrays. *Macromol.*, 40:3749-3756, 2007. c) R. K. Shah, J.-W. Kim and D. A. Weitz. Monodisperse Stimuli-Responsive Colloidosomes by Self-Assembly of Microgels in Droplets. *Langmuir*, 26:1561-1565, 2010.

# List of Abbreviations

| | |
|---|---|
| BIS | *N,N'*-methylenebis(acrylamide) |
| CLSM | Confocal laser scanning microscopy |
| DLS | Dynamic light scattering |
| KPS | Potassium persulfate |
| LCST | Lower critical solution temperature |
| MRB | Methacryloxyethyl thiocarbamoyl rhodamine B |
| NIPAM | *N*-isopropylacrylamide |
| NIPMAM | *N*-isopropylmethacrylamide |
| FITC | Fluorescein isothiocyanate |
| PNIPAM | Poly-*N*-isopropylacrylamide |
| PNIPMAM | Poly-*N*-isopropylmethacrylamide |
| PDMS | Polydimethylsiloxane |
| SAXS | Small angle X-ray scattering |
| SANS | Small angle neutron scattering |
| SDS | Sodium dodecyl sulfate |
| SLS | Static light scattering |
| V50 | 2,2'-azobis(2-methylpropionamidine) dihydrochloride |
| VPTT | Volume phase transition temperature |

# Contents

# Chapter 1

# Introduction

## 1.1 Introduction

(Spherical) colloidal particles have an undefined valency and interacts with each other in all possible directions. However, so-called colloidal molecules are analogous to atomic molecules and share with those properties such as specific valency and directional bonding. The expression, colloidal molecules, was first coined by van Blaaderen [1]. Colloidal molecules have been created in several different ways. For example, Wang *et al.* produced colloidal molecules from styrene particles functionalized with DNA patches that could act as binding sites for particles carrying complementary DNA [2]. Sacanna *et al.* formed colloidal molecules by taking advantage of depletant-induced lock-and-key interactions between particles with complementary shape [3]. Xia *et al.* used lithographically patterned templates to form aggregates of polystyrene particles with specific valency and geometry as determined by the template design [4]. Kraft *et al.* achieved colloidal molecule-like clusters through the coalescence of liquid protrusions on various polymers seeds [5]. Finally, Manoharan *et al.* formed clusters of hard spheres from particle-stabilized emulsions with subsequent evaporation of the dispersed phase [6]. Kim *et al.* also used a particle-stabilized emulsion approach, where patchy particles were obtained by solidification of the oil phase [7].

The aim of this project was to synthesize thermoresponsive colloidal molecules by clustering of microgel particles based on either poly(*N*-isopropylacrylamide) (PNIPAM) and poly(*N*-isopropylmethacrylamide) (PNIPMAM). Microgels are cross-linked hydrogel particles in the nanometer to micrometer scale and are thermoresponsive with respect to size, charge density and interaction potential. Because of the externally tunable properties of microgels, they are in several respects more interesting to study compared to traditional hard spheres.

In this project, amine-functionalized PNIPAM and PNIPMAM microgel particles were synthesized by co-polymerization with allylamine. Functionalization with amine groups allows for microgel-microgel cross-linking in the presence of glutaraldehyde (Figure 1.1 A). Cross-linking is a requirement for microgel clusters to remain intact when dispersed in water. The synthesis project was inspired by work by Huang *et al.*, Shah *et al.* and James *et al.* [8, 9, 10] in which amine groups were utilized to cross-link microgels with glutaraldehyde. The cross-linking ability of the synthesized microgels was first demonstrated in bulk by addition of glutaraldehyde to concentrated microgel suspensions. A droplet-based microfluidics approach was then used in an attempt to form colloidal molecule-like microgel clusters with glutaraldehyde bridges covalently holding the clusters together (Figure 1.1 B). The ultimate goal was to form clusters with two different microgels, one PNIPAM and one PNIPMAM, distinguishable by different colors. This

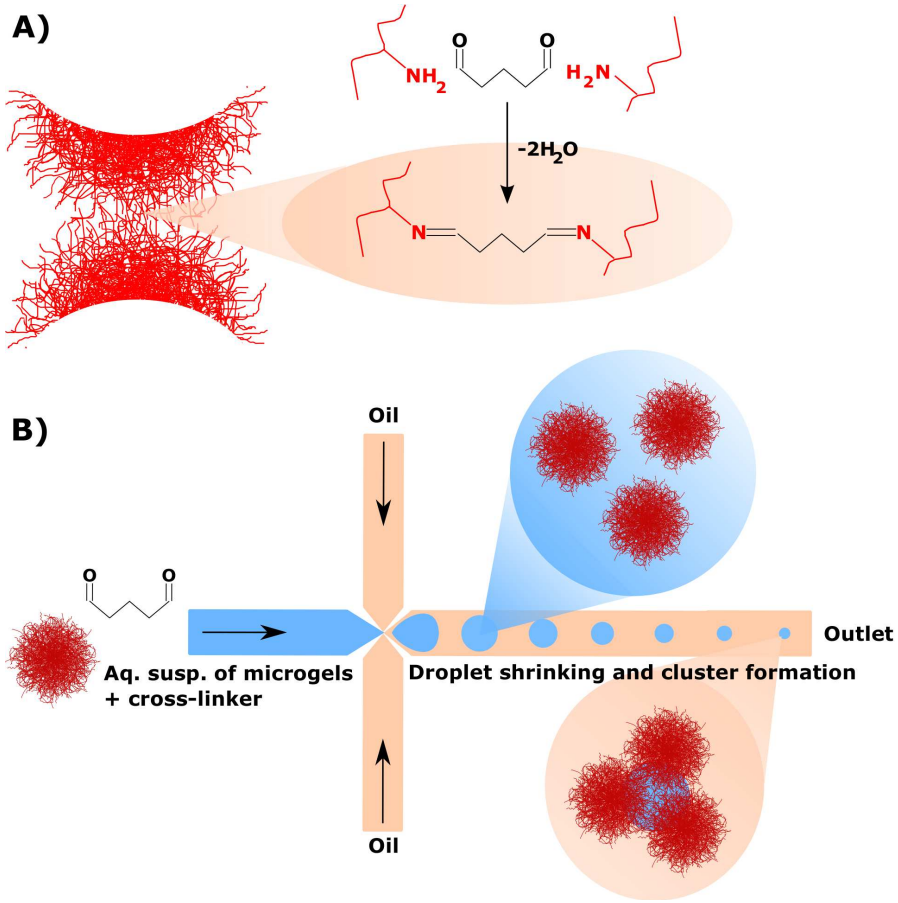


Figure 1.1: A) Microgel-microgel cross-linking between amine groups on the microgels' surface can be achieved with glutaraldehyde. B) Strategy for obtaining colloidal molecule-like microgel clusters by droplet-based microfluidics.

would give colloidal molecules with two different kinds of interaction sites, both thermoresponsive, but with different thermoresponsive behavior.

# Chapter 2

# Theory

## 2.1 Colloids

Colloidal particles, or colloids, are particles in the nanometer to micrometer scale that are dispersed in any kind of medium, i.e. a dispersion medium [11]. Because of their small size, they possess a large surface-to-volume ratio. The large surface area of colloids means that the interface between a colloid and the surrounding dispersion medium plays a key role in particle stability; a larger surface means more interactions between the colloid and the dispersion medium. This interaction is unfavorable in general, as the dispersion medium most often prefer to interact with itself. This effect favors aggregation of particles, thus decreasing the surface area and as a result the free energy of interaction. Colloids are stabilized in two primary ways, steric and electrostatic stabilization. Both mechanisms of stabilization are based on an osmotic effect, where the approach of two particles gives an increase in counterion or polymer density between the particles, respectively, which results in a flow of solvent into the area that drives the particles apart. With steric stabilization there is an additional entropic effect, which the approach of two particles being disfavoured due to limitations in the number of conformations that the adsorbed or grafted polymers can adopt. The overall stability is a balance between the attractive dispersion interactions coupled with the desire to decrease the surface area and the repulsive steric and electrostatic interactions[12].

## 2.2 Microgels

### 2.2.1 Introduction to microgels

Microgels are colloidal, water swollen, cross-linked hydrogel particles. In the polymerization process, the cross-linker is consumed more rapidly than the monomer which results in an uneven distribution of cross-linker within the microgel particles (Figure 2.1). More cross-linker is found in the particle core than in the shell and thus the core is more dense than the exterior shell. At low temperatures, the interaction between the constituent polymer and water is favored, and the particles are large and water-swollen. However, as the temperature increases, water progressively becomes a bad solvent for the polymer and the polymer-polymer interactions become more favorable. When the polymer-polymer interactions dominate, the particles shrink and discharge water, thereby decreasing the interaction energy (Figure 2.2). As the size of the particles decreases, the density as well as the charge density increases. The narrow temperature range in

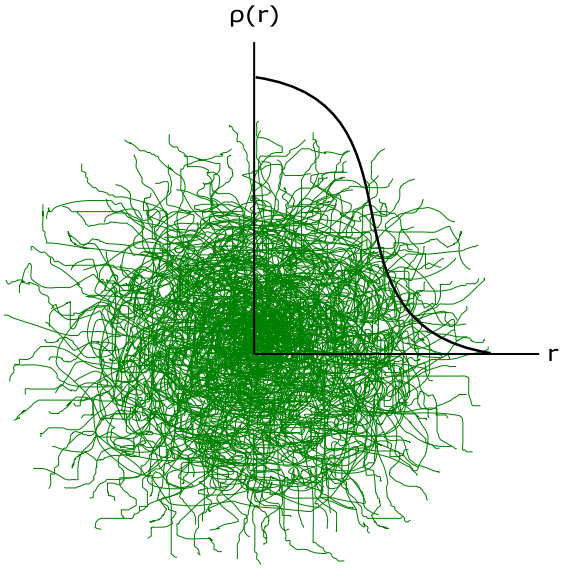


Figure 2.1: Microgel density profile.

which the particles shrink is known as the volume phase transition temperature (VPTT) [13]. The VPTT depends on the identity of the polymer.

### 2.2.2 Stability of microgels

Like with all colloidal particles, the stability of microgels is dependent on the presence of steric and electrostatic stabilization as described in section 2.1. Below the VPTT, the particles are large and water swollen with a relatively low charge density (Figure 2.2). In this regime the particles have dangling polymer chains extending from the surface, providing steric stabilization. At temperatures above the VPTT, these chains are collapsed into the core and steric stabilization is lost. However, as the particles become smaller they possess a significantly larger charge density, making the stabilization mainly electrostatic [14]. Presence of salt in a microgel suspension above the VPTT screens the electrostatic repulsion between microgel particles and thus induces aggregation at sufficiently high salt concentrations. However, below the VPTT, where steric stabilization is in play, the suspension is unaffected by addition of salt [14].

### 2.2.3 Microgel synthesis

Microgels are commonly synthesized using a method called free radical precipitation polymerization [13] where an ionic radical initiator is added to a monomer solution at elevated temperature. At elevated temperature the initiator thermally decomposes and forms radicals that initiate polymerization of the monomers. Because of the lower critical solution temperature (LCST) of *N*-isopropylacrylamide (NIPAM) and *N*-isopropylmethaacrylamide (NIPMAM) polymers, their solubility decreases at higher temperatures. When the polymers have reached a certain size they therefor precipitate out of the solution. When precipitated, the polymer radicals react with each other, or with other monomers, forming larger polymer particles. Eventually the particles reach a size where they are colloidally stable due to the surface charges introduced by the ionic initiator [13]. The initiator can be either cationic or anionic and the charge of the initiator

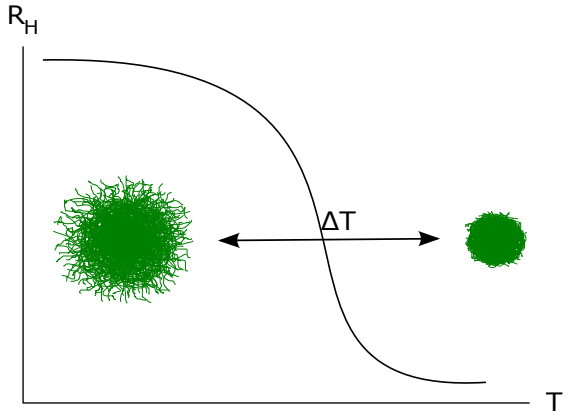


Figure 2.2: Below the VPTT, microgels are large and water-swollen. Above the VPTT, where water is a bad solvent for the polymer, microgels are collapsed.

will largely determine the charge of the microgel particles. In order to prevent the gel from completely dissolving in water, a cross-linker is co-polymerized to form a polymer network. The cross-linker is consumed faster than the monomer which gives particles with a denser core and a more fuzzy shell (Figure 2.1). Surfactant can be used in the synthesis to promote the formation of smaller particles by stabilizing them at a smaller size. Alternatively, the amount of cross-linker can be varied. Functional groups can be added to the microgels by co-polymerization with a polymerizable monomer that contain said group, for example allylamine to add amine groups.

## 2.3 Microfluidics

In droplet-based microfluidics, the goal is to create small, relatively monodisperse droplets of a dispersed fluid. Droplets are formed in the junction between two streams of immiscible liquids by injecting a discrete phase, i.e. the sample, into a stream of the continuous medium and thereby utilizing the interfacial tension to form spherical droplets. The size of the droplets is controlled by the size of the junction where the two phases meet - the droplets will not be smaller than the junction - and the shear force of the two mediums. The shear force is in turn determined by the pressure that is applied to the inlets where the mediums are injected.

If the sample contains colloidal particles, the contents of the droplets can be controlled through the droplet size and the number density of the particles. The number of particles in the droplets can be described by a Poisson-distribution. The size of the droplets and the concentration of the suspension can be chosen so that the maximum probability in the distribution corresponds to the number of particles desired in each droplet. In this way the number of droplets containing the desired amount of particles is maximized.

## 2.4 Characterization techniques

### 2.4.1 Confocal laser scanning microscopy

In confocal laser scanning microscopy (CLSM) the sample is excited by a monochromatic laser beam that illuminates a single point in the sample. The light is collected through a pinhole which only lets through light that comes from the plane that lies confocal to the pinhole. This

means that one can look at a thin slice of the sample at a time. Removing the out-of-plane light results in increased contrast as well as resolution, yielding clearer pictures compared to ordinary wide-field microscopy. If confocal microscopy is performed on multiple planes throughout the sample, the two-dimensional pictures can be combined to create a three-dimensional image of the sample. The transmitted light is collected using a photon counting detector; the sensitivity of these detectors can be optimized on sample to sample basis. Due to the nature of the point by point excitation, highly dynamic samples with a lot of movement will result in lower quality images.

### 2.4.2 Light scattering for size determination

#### 2.4.2.1 Static light scattering

When light hits a sample, the sample will scatter light in all directions based on the difference in refractive index between the particles and the solvent. The intensity of the scattered light depends on the volume of sample hit by the laser, i.e. the scattering volume, the size of the scattering particles as well as the wavelength of the light used, $\lambda$. In the static light scattering (SLS) experiment, the intensity of the scattered light is measured as a function of the scattering angle, $\theta$. The scattering angle is related to the so called scattering vector, $q$:

$$q = \frac{4\pi}{\lambda} \sin(\frac{\theta}{2}) \tag{2.1}$$

In SLS, the measured intensity of the scattered light is plotted as a function of $q$. The curve obtained can be fitted with software to obtain data about the particles, such as size and polydispersity. The measured data is a combination of inter- and intra-particle scattering effects. The scattering from a single particle is referred to as the form factor and the inter-particle effects, based on particle-particle interactions, are described by the structure factor. If the concentration of the sample is sufficiently low, the particles can be considered non-interacting and the structure factor is unity.

#### 2.4.2.2 Dynamic light scattering

In the dynamic light scattering (DLS) experiment as opposed to the static, the scattered intensity is measured as a function of time at a single angle. The intensity of the scattered light fluctuates over time as the particles move in the sample. From this data, a correlation function, $g_2(\tau)$, that describes the movement of particles in the sample over the time, $\tau$, is acquired. The correlation function includes a decay rate, $\Gamma$, which describes how quickly the correlation function approaches zero. The relationship between the correlation function and the decay rate is given by:

$$\sqrt{g_2(\tau) - 1} = Ae^{\Gamma\tau} \tag{2.2}$$

where $A$ is an experimental coefficient that depends on experiment setup and laser coherence. The decay rate is related to the scattering vector, $q$, as well as the diffusion coefficient, $D$, of the particles in the sample:

$$\Gamma = q^2 D \tag{2.3}$$

The decay rate is larger for particles with faster diffusion and as a result the correlation function decays faster for smaller particles compared to large for which the diffusion is slower. The two equations can be combined and rewritten so that the diffusion coefficient can be obtained:

$$\ln \sqrt{g_2(\tau) - 1} = \ln A + q^2 D\tau \tag{2.4}$$

According to this expression the diffusion coefficient can be obtained by plotting $\ln \sqrt{g_2(\tau) - 1}$ versus time, $\tau$. The diffusion coefficient can then be converted to a hydrodynamic radius, $R_H$, by the Stokes-Einstein relation, assuming that the particles are spherical:

$$R_H = \frac{kT}{6\pi\eta D} \tag{2.5}$$

### 2.4.3 Electrophoretic mobility measurements

The electrophoretic mobility, $\mu$, of a colloidal particle describes how fast the particle is moving under the influence of an electric field, $\vec{E}$. The measured velocity, $\vec{v}$, depends on the force applied from the electric field, $\vec{F}$, the viscosity, $\eta$, of the medium as well as the radius of the particles, $R$. This is described by Stoke's law:

$$\vec{v} = \frac{\vec{F}}{6\pi\eta R} \tag{2.6}$$

The electrophoretic mobility is then defined as:

$$\mu = \frac{\vec{v}}{\vec{E}} \tag{2.7}$$

In the case of an isolated particle, the force applied is proportional to both the applied electric field and the charge of the particle, $q$ [15]:

$$\vec{F} = q\vec{E} \tag{2.8}$$

Combining these three equations gives a new expression for the electrophoretic mobility of a single particle:

$$\mu = \frac{q}{6\pi\eta R} \tag{2.9}$$

The electrophoretic mobility increases with increasing charge density. Electrophoretic mobility can thus be used as a measure of particle charge.

# Chapter 3

# Materials and Methods

## 3.1 Microgel synthesis

### 3.1.1 General

All chemicals were purchased from commercial chemical suppliers and were used without further purification. Milli-Q water (18.2 MΩ·cm) was used for all synthesis reactions, purifications, solution preparations and emulsifications. Reactions were carried out in room temperature.

### 3.1.2 Microgel synthesis procedure

**General procedure.** To a three-necked round bottom flask (500 ml) in a temperature controlled water bath was added NIPAM or NIPMAM monomer (3.0 g), BIS cross-linker (0.21 g or 0.18 g, 5 mol% with respect to NIPAM or NIPMAM), allylamine (199 $\mu$L or 177 $\mu$L, 10 mol% with respect to NIPAM or NIPMAM), sodium dodecyl sulfate (40 mg, 13 mg/g monomer), a solution of MRB (4 mg dissolved in 3 ml Milli-Q water, 0.022 and 0.024 mol% with respect to NIPAM and NIPMAM) or FITC (27 mg in 20 ml Milli-Q water, 0.26 and 0.29 mol% with respect to NIPAM and NIPMAM) dye, and Milli-Q water (180.0 ml). The FITC solution was prepared by reacting FITC (27 mg) and allylamine (72 $\mu$L, 1380 mol% with respect to FITC) in a NaOH-solution (20 ml, $10^{-4}$ M) under a nitrogen atmosphere over night. The three-necked round bottom flask was then fitted with a magnetic stir bar, a reflux condenser, a nitrogen gas inlet and a septum. The reaction mixture was heated to 60°C under a stream of nitrogen and with constant stirring for 1 hour, after which the temperature was increased to 70°C. A degassed solution of KPS or V50 initiator (0.135 g, 1.88 or 2.12 mol% with respect to NIPAM and NIPMAM, in 20 ml of Milli-Q water) was then added dropwise, upon which an increase in turbidity was observed. After 4 hours, the reaction mixture was cooled to 40°C and was subsequently filtered through glass wool to remove particulate matter. The obtained microgel suspension was purified by dialysis, using a dialysis membrane with a cut-off value of 12000-14000 g/mol, for at least 7 days with water being changed 3 times per day. Concentrated microgel suspensions were obtained by repeated centrifugation using a Sigma 3k30 centrifuge, with subsequent decantation of the supernatant, or alternatively by freeze-drying and redispersion. In total, nine syntheses were performed with variations in polymer, dye, initiator and amount of surfactant and cross-linker added, described in the Table 3.1.

Table 3.1: Overview of synthesized microgel systems LE1-LE9.

| Batch | Monomer | Initiator | Dye | SDS (mg/3 g monomer) | BIS (mol%) |
|---|---|---|---|---|---|
| LE1 | NIPAM | KPS | MRB | 40 | 5.0 |
| LE2 | NIPMAM | KPS | FITC | 40 | 5.0 |
| LE3 | NIPAM | KPS | MRB | 0 | 5.0 |
| LE4 | NIPAM | KPS | MRB | 20 | 5.0 |
| LE5 | NIPAM | V50 | MRB | 20 | 5.0 |
| LE6 | NIPAM | V50 | MRB | 40 | 5.0 |
| LE7 | NIPMAM | KPS | MRB | 40 | 5.0 |
| LE8 | NIPAM | KPS | FITC | 40 | 5.0 |
| LE9 | NIPAM | KPS | MRB | 40 | 1.3 |

## 3.2 Microgel characterization techniques

### 3.2.1 Confocal laser scanning microscopy

Confocal micrographs were recorded on a Leica SP5 confocal laser scanning microscope mounted in a thermostated enclosure and operated in the inverted mode (D6000I), using a 100x /1.4 NA immersion objective. The suspensions were kept between two cover glasses separated by a 120 $\mu$m spacer. Covalent incorporation of fluorescent rhodamine or fluorescein derivatives during microgels synthesis enabled fluorescence CLSM studies of microgels. A 488 nm Ar ion and a 543 nm HeNe laser were used to excite the red fluorescence of rhodamine B (543 nm) and the green fluorescence of fluorescein (488 nm), respectively. Samples were studied at 20°C unless otherwise stated.

### 3.2.2 Light scattering measurements

#### 3.2.2.1 General instrumentation

Static- and dynamic light scattering (SLS and DLS) was performed using a 3D LS instrument which implements a HeNe laser light source (632.8 nm, 35 mW). The intensity of the scattered light was measured relative to the transmitted beam using two Avalanche Photodiodes and was processed by a Flex correlator in a 3D cross-correlation configuration with modulation unit [16]. 5 mm cylindrical NMR-tubes were used as sample cells. Temperature control of the sample was ensured by regulating the vat temperature using a water circulation thermostat. The temperature was controlled with an accuracy of 0.1°C.

#### 3.2.2.2 Static light scattering

The angular dependence of the intensity of the scattered light was measured at angles from 30 to 110° at every 2°. At each angle one measurement of 60 seconds was performed. The corrected intensity, $I_{final}$, was plotted versus the scattering vector, $q$. Measurements were carried out at 20, 30, 40 and 50°C. Microgel suspensions with concentrations of $10^{-1}$ wt% were used in all light scattering experiments.

#### 3.2.2.3 Dynamic light scattering

The fluctuations in the intensity of the scattered light was measured at an angle of 45°. The hydrodynamic radius, $R_H$, was calculated from the obtained correlation function through a first

order cumulant analysis. $R_H$ is given as the average over five consecutive measurements of 180 seconds. Microgel swelling curves were obtained by measuring $R_H$ as a function of temperature in the range 20 to 55°C.

### 3.2.3 Electrophoretic mobility measurements

A Malvern ZetaSizer Nano-Z equipped with a HeNe laser with automatic laser attenuator was used for measurements of electrophoretic mobility of microgels. Disposable folded capillary cells were used as samples cells. Measurements were preformed at a fixed scattering angle of 17° using a laser interferometric technique (laser Doppler electrophoresis) which enables the determination of the electrophoretic mobility. The electrophoretic mobility is given as the average of 10 consecutive measurements. Microgels were measured from 20 to 55°C in steps of 5°C. At each temperature, samples were equilibrated for 20 minutes prior to measurements. Microgel suspensions with concentrations of $10^{-1}$ wt% were used.

## 3.3 Temperature dependent interaction potential

LE2 microgel suspension (450 $\mu$L, 3.6 wt%) was added to three Eppendorf tubes. KCl solution (1 M, 50 $\mu$L) was added to two of the tubes, and glutaraldehyde solution (50 $\mu$L, 50 wt%) was added to one of these two tubes. To the third tube only mili-Q water (50 $\mu$L) was added. The samples were vortexed before imaging by CLSM. Images were recorded at 20 and 50°C, as well as at 30°C on cooling down. Sample equilibration time was 30 minutes.

## 3.4 Microgel-microgel cross-linking

LE1, LE2, LE7 and LE9 microgel suspensions were concentrated by centrifugation and decantation to obtain dense pellets. Glutaraldehyde (50 $\mu$L, 50 wt%) was then added to the top of the pellets and the samples were left to cross-link for a minimum of 4 days to allow for the reaction to be completed. The formed gels were placed in water for one week to confirm successful cross-linking.

## 3.5 Cross-linking of microgel fractals

LE2 microgel suspension (3.6 wt%, 450 $\mu$L) was added to two Eppendorf tubes. To one of the tubes was added KCl solution (1 M, 50 $\mu$L) and glutaraldehyde solution (50 wt%, 50 $\mu$L) – to the other one just Milli-Q water (50 $\mu$L). The contents of the tubes were vortexed, and the tubes were then placed in a heating chamber (Fratelli Galli Micro Incubator M91) at 50°C for 3 days. Upon cooling back to 20°C and after several hours of equilibration, the suspensions were studied by CLSM.

## 3.6 Microfluidics

All microfluidics devices used were created by soft lithography from polydimethylsiloxane (PDMS). The devices had one sample inlet, one inlet for the continuous phase, two outlets as well as permeable walls to allow for droplet shrinking and microgel cluster formation. A mixture of microgel suspension (0.025 wt%) and glutaraldehyde (20 $\mu$L, 50 wt%) was used as sample and Fluorinert FC-40 oil was used as the continuous phase. The flow rates used were 750 and 600 $\mu$L/h for the

continuous and dispersed phases respectively, but were optimized for each experiment separately. The flow rates were controlled using a Fluigent flow rate control unit, with a maximum pressure of 1000 mbar. The experiment was followed using an inverted fluoresence microscope (Nikon Te-2000U) and a mikrotron high speed camera.

The output oil was collected and was left to allow for microgel-microgel cross-linking for at least 48 hours before attempting to extract clusters. After 48 hours water was added to the sample after which it was centrifuged. Pico Break surfactant was then added before the sample was centrifuged again. Finally, the water phase was collected and characterized.

# Chapter 4

# Results and Discussion

The aim of this project was to create colloidal molecules by clustering of amine-functionalized poly-*N*-isopropylacrylamide (PNIPAM) and poly-*N*-isopropylmethacrylamide (PNIPMAM) microgel particles using glutaraldehyde to form microgel-microgel cross-links that hold the colloidal molecules together. For this purpose, several microgel systems were synthesized and characterized. The most promising of these microgels were then utilized in droplet-based microfluidics to create colloidal molecule-like microgel clusters. This chapter will first deal with the synthesis and characterization of microgels and secondly with their assembly into colloidal molecules.

## 4.1 Microgel synthesis and characterization

### 4.1.1 Synthesis procedure

PNIPAM and PNIPMAM microgels were synthesized by free radical precipitation polymerization using *N*-isopropylacrylamide (NIPAM) and *N*-isopropylmethacrylamide (NIPMAM) as main monomers and *N*,*N*'-methylenebisacrylamide (BIS) as a cross-linker. BIS carries two polymerizable acrylamide groups that can form cross-links between two polymer chains, effectively yielding a polymer network. Potassium persulfate (KPS) and 2,2'-azobis(2-methylpropionamidine) dihydrochloride (V50) were used as initiators. Those are thermal, ionic initiators that decompose to radicals at temperatures above 70°C. In the polymerization process, the initiator residuals become incorporated at the ends of the polymer chains and thereby confer their charge to the formed microgel particles. KPS is an anionic initiator, which gives negatively charged polymers, and V50 is a cationic initiator that gives positively charged polymers. The fluorescent dyes methacryloxyethyl thiocarbamoyl rhodamine B (MRB) and fluorescein isothiocyanate (FITC) were covalently incorporated in the polymers by co-polymerization to enable fluorescent confocal laser scanning microscopy (CLSM) studies. In order for FITC to be incorporated, it had to be coupled to allylamine prior to the reaction; allylamine provides FITC with a polymerizable double bond. Finally, the monomers were co-polymerized with allylamine to functionalize the microgels with amine groups. 10 mol% of allylamine was used in all cases to create a sufficient amount of amine groups on the surface of the microgel particles, thereby ensuring that they can later be inter-cross-linked by glutaraldehyde.

The syntheses were carried out in a three-necked round bottom flask fitted with a nitrogen gas inlet, a reflux condenser and a septum, through which the initiator was added (Figure 4.1). In total nine syntheses were completed - as summarized in Table 4.1 - and the obtained systems were given the names LE1-LE9. The syntheses were inspired by work by Huang *et al.*, Shah *et*

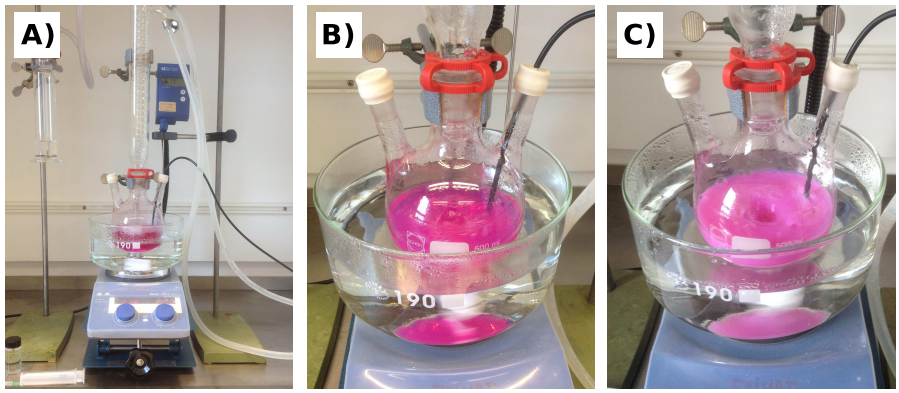


Figure 4.1: A) Microgel synthesis setup. On addition of initiator, the solution went from clear (B) to turbid (C).

*al.* and James *et al.* [8, 9, 10].

Table 4.1: Overview of synthesized microgel systems LE1-LE9. Syntheses was carried out on a 3 gram scale. If no note, the procedure was successful.

| Batch | Monomer | Initiator | Dye | SDS (mg) | BIS (mol%) | Note |
|---|---|---|---|---|---|---|
| LE1 | NIPAM | KPS | MRB | 40 | 5.0 | - |
| LE2 | NIPMAM | KPS | FITC | 40 | 5.0 | - |
| LE3 | NIPAM | KPS | MRB | 0 | 5.0 | Phase separation |
| LE4 | NIPAM | KPS | MRB | 20 | 5.0 | Phase separation |
| LE5 | NIPAM | V50 | MRB | 20 | 5.0 | Phase separation |
| LE6 | NIPAM | V50 | MRB | 40 | 5.0 | Phase separation |
| LE7 | NIPMAM | KPS | MRB | 40 | 5.0 | - |
| LE8 | NIPAM | KPS | FITC | 40 | 5.0 | Phase separation |
| LE9 | NIPAM | KPS | MRB | 40 | 1.3 | - |

All of the performed syntheses were done on a 3 g scale, except for LE6 which was halved. Two complementary systems were first synthesized, red PNIPAM and green PNIPMAM (LE1 and LE2). As a starting point, 40 mg of sodium dodecyl sulfate (SDS) was added and KPS was used as initiator. The LE1 particles were somewhat too small to be properly resolved by CLSM and in order to obtain larger particles SDS was removed from the following synthesis (LE3). SDS provides steric stabilization for the particles which results in them becoming stable at a smaller radius during the polymerization process. A smaller amount of SDS will therefore, theoretically, increase the particle radius. However, exclusion of SDS resulted in major phase separation during synthesis, essentially forming a macrogel instead of a microgel. Following LE3, the procedure was repeated but with half the original amount of SDS (LE4). This fourth synthesis had the same outcome as the preceding synthesis, with major phase separation. In the following syntheses (LE5 and LE6), the anionic KPS initiator was replaced with the cationic V50 initiator. It was assumed that the negative charges conferred by KPS could interfere with and partially cancel out the charges originating from the amine groups, thus giving poor charge stabilization of the particles. It was hypothesized that this problem could be circumvented by using a positively charged initiator. Both syntheses using V50 as initiator failed, at both 20 mg and 40 mg of added SDS (LE5 and LE6, respectively). The limited amount of time at disposal prompted the syntheses of the complementary systems to the first two. Thus, a red PNIPMAM (LE7)

Figure 4.2: Iridescence observed for LE1 at 3.6 wt%.

and a green PNIPAM (LE8) were synthesized, only changing the dye used with respect to LE1 and LE2. LE8 started to partly phase separate as the temperature was lowered upon complete synthesis. After removal of the aggregates by filtration, a low yield of polydisperse and clustered microgels was obtained. Finally, it was attempted to reproduce the synthesis of Huang *et al.* who obtained microgel particles with a hydrodynamic radius of 300 nm using 40 mg SDS and with a lower amount of cross-linker added (LE9) [8]. Successfully obtained microgel systems LE1, LE2, LE7 and LE9 were purified by dialysis against mili-Q water. To concentrate the microgel suspensions, they were centrifuged and the supernatant was removed. The sedimentation rate of LE9 was however slow, likely due to the low density of the particles, and to obtain a concentrated suspension it was freeze dried and then resdispersed in water.

Concentrated microgel suspensions of LE1, LE2 and LE7 ($\sim$ 3.5 wt%) showed iridescence at the wall of the plastic storage tubes (Figure 4.2). The iridescence stems from Bragg diffraction due to formation of highly ordered crystalline domains in the sample. The regular distances between the particles act as a grating for light, analogous to the diffraction of X-rays by a true crystal, but the larger distances in colloidal crystals means that the affected wavelength lies in the visible region. Monodisperse particles form ordered arrays easier than polydisperse ones because of irregularity in the inter-particle distance introduced by the size difference. The formation of crystalline domains in the samples is thus indicative of high particle monodispersity.

### 4.1.2 Microgel characterization

#### 4.1.2.1 Confocal laser scanning microscopy

FITC and MRB dyes were co-polymerized into the polymer network of the microgel particles to enable fluorescence CLSM studies. To make imaging easier and in order to obtain higher quality images, microgels were studied when adsorbed to the cover slip, where they are essentially stationary. Microgels adsorb to glass surfaces due to hydrogen bonding between glass hydroxyl groups and amide groups in the microgels' polymer chains. In addition, the transmission drastically decreases deeper in the sample and thus less light can be collected by the detector. With LE2 and LE7, individual microgels could clearly be resolved. However, in terms of size, LE1 and LE9 microgel particles appeared to be at the limit of what can be resolved by the CLSM instrument. CLSM micrographs of dilute suspensions (1 wt%) of LE2 and LE7 are shown in

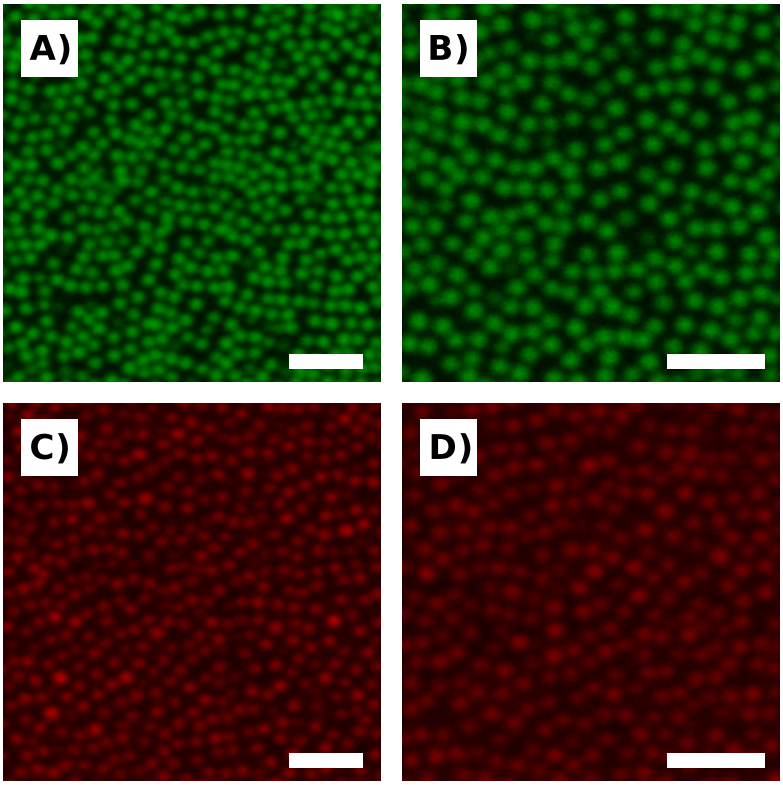


Figure 4.3: Fluorescence CLSM micrographs of 1 wt% microgel suspensions LE2 (A and B) and LE7 (C and D) imaged at the cover slip.

Figure 4.3. From the micrographs it can be concluded that the microgels are dyed and appear monodisperse. In addition, LE2 microgels were studied by CLSM at higher concentration (4.7 wt%) (Figure 4.4). According to the micrographs, the microgels arrange into hexagonal, crystalline arrays, with only a few crystal defects present. As previously mentioned, the crystalline behavior points to high particle monodispersity. However, the microgels were studied in the absence of salt, which facilitates crystal formation. Traditionally, micrographs are recorded at a minimum distance of ten $\mu$m from the cover slip to minimize wall effects. However, due to the high concentration of the suspension and to the confocal pinhole, transmission rapidly decreased deeper in the sample. Consequently, to be able to record good-quality images, the microgels were studied five $\mu$m away from the cover slip. Anyhow, due to the small size of the microgel, five $\mu$m is several particle layers away from the glass surface so wall effects should still be small. The crystalline regime of LE7 has not yet been explored, but will be subject for later studies.

#### 4.1.2.2 Dynamic light scattering

The hydrodynamic radius ($R_H$) of the microgel particles was determined by dynamic light scattering (DLS) measurements at a single angle of 45°, and using a first order cumulant analysis. The single angle and first order cumulant analysis was considered sufficient because of the apparent particle monodispersity. The thermoresponsive behavior of the microgels - with respect to size - was studied by measuring the $R_H$ as a function of temperature (Figure 4.5 A). The measurements were carried out in the range of 20-50°C for PNIPAM and 20-55°C for PNIP-

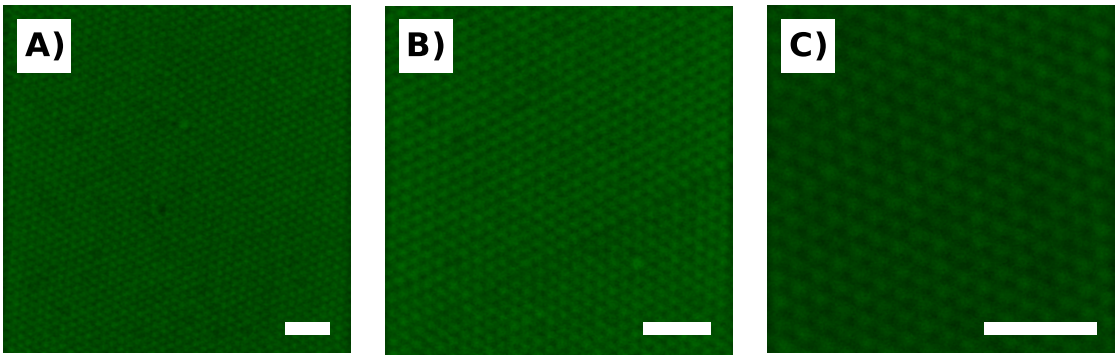


Figure 4.4: LE2 microgels (4.7 wt%) imaged by fluorescence CLSM at 20°C. Scale bars are 2 $\mu$m.

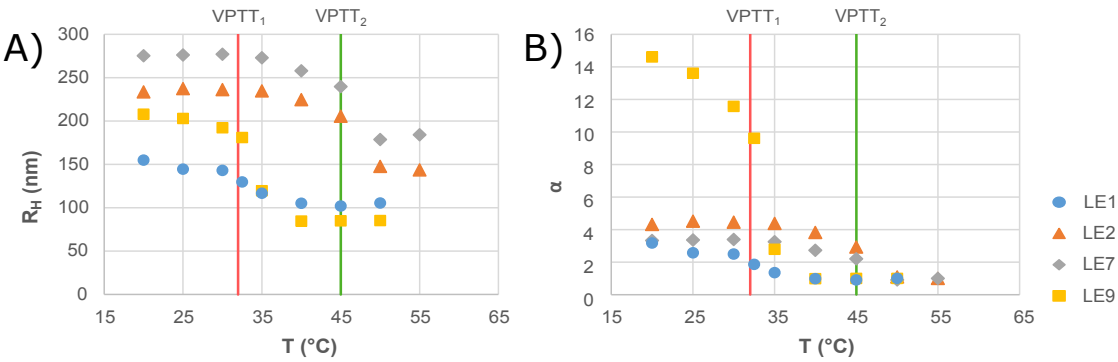


Figure 4.5: Temperature dependence of A) the hydrodynamic radius, $R_H$, and B) the swelling ratio, determined by DLS for LE1, LE2, LE7 and LE9. The vertical lines show the theoretical VPTT of PNIPAM ($VPTT_1$) and PNIPMAM ($VPTT_2$), respectively.

MAM. Due to the lower critical solution temperature (LCST) of PNIPAM and PNIPMAM, the microgels are expected to undergo a volume transition as the temperature is increased and the solvent becomes progressively bad. The volume phase transition temperature (VPTT) is expected to occur at 32°C for PNIPAM and 45°C for PNIPMAM. The VPTT is slightly shifted in our measurements, possibly due to the presence of amine groups. The difference is small and does not appear significant, however.

As previously mentioned, the synthesis of LE9 was a replica from Huang *et al.* who obtained 300 nm radius particles [8]. However, the repeated procedure yielded particles of just 200 nm. The difference in size can be attributed to differences in for example water amount, chemical purity, stirring, efficiency of degassing or temperature variations.

#### 4.1.2.3 Swelling ratio

From the DLS measurements, the temperature dependence of the microgel swelling ratio could be obtained (Figure 4.5 B). The swelling ratio, $\alpha$, is defined as:

$$\alpha = \frac{R_{H,T}^3}{R_{H,c}^3} \tag{4.1}$$

where, $R_{H,T}$, is the hydrodynamic radius at a given temperature $T$ and $R_{H,c}$ is the hydrodynamic radius in the fully collapsed state. The $\alpha$-versus-$T$ curves for LE2 and LE7 are alike as is expected

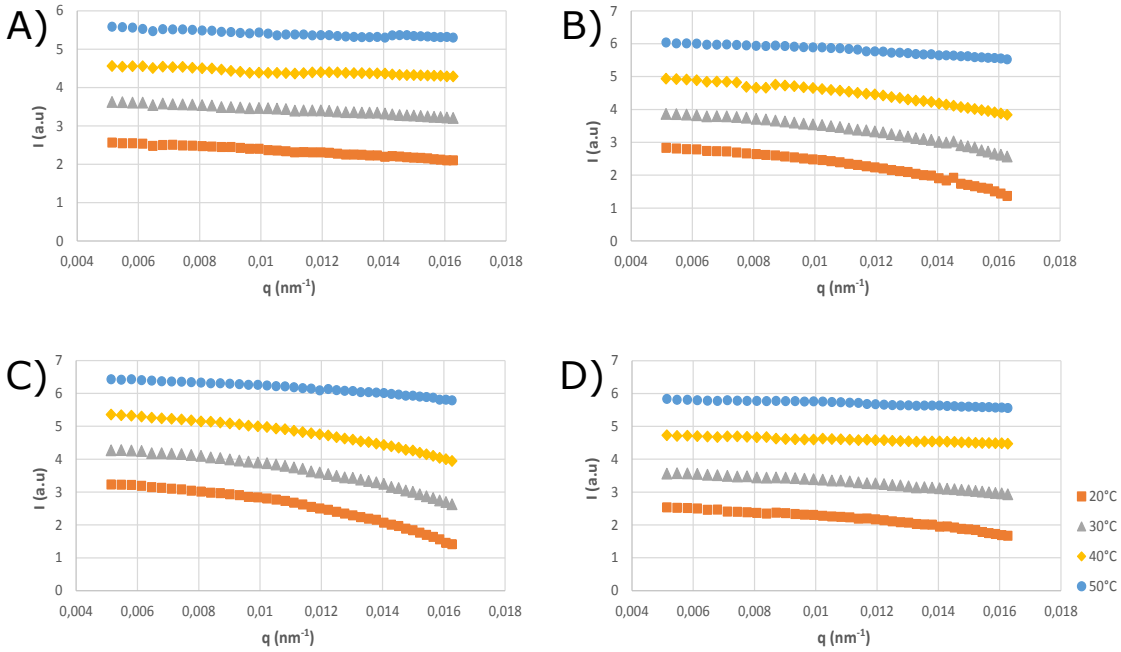


Figure 4.6: Data obtained from SLS measurements: scattered intensity, I, plotted versus the scattering vector, q, for A) LE1, B) LE2, C) LE7 and D) LE9.

since the only difference between them is the dye used; the cross-linking density is the same and both are PNIPMAM-based. LE1 have similar swelling ratios to LE2 and LE7, with the difference in VPTT attributed to the different polymer. The swelling ratio at 20°C is essentially the same for LE1, LE2 and LE7, with all of them having the same cross-linking density. However, LE9 has a significantly higher swelling ratio at 20°C, between three and four times larger than the others. The difference can be attributed to the roughly four times smaller cross-linking density. A less cross-linked particle have a greater ability to swell and therefore absorbs more water.

#### 4.1.2.4 Static light scattering

In static light scattering (SLS), the intensity of the scattered light was measured in the angular range of 30-110° with an increment of 2°. The microgel particle thermoresponsivity was studied by performing measurements at 20, 30, 40 and 50°C (Figure 4.6). However, the microgel particles are too small to display a minimum in the form factor in the accessible $q$-range and consequently no information about the size could be obtained. In order to obtain the size by fitting of the form factor, small angle scattering techniques, such as small angle X-ray scattering (SAXS) or small angle neutron scattering (SANS), could be used to probe form factor minima.

#### 4.1.2.5 Electrophoretic mobility

Particle charge was determined by measuring the electrophoretic mobility of the microgels (Figure 4.7). Normally, the charge of a microgel particle arises largely from residuals of the ionic initiator used to initiate the polymerization during microgel synthesis. However, in this case the microgels have amine groups incorporated, that will confer a positive charge when protonated. Protonated amine groups are in equilibrium with unprotonated amine groups. This equilibrium

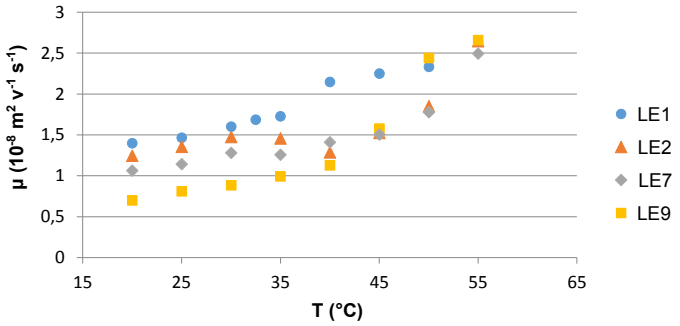


Figure 4.7: Temperature-dependent electrophoretic mobility for LE1, LE2, LE7 and LE9.

is at neutral pH shifted towards the protonated amine ($pK_a \sim 10$). The charge conferred by the amine groups is relatively small but still present. The electrophoretic mobility was measured as a function of temperature and thus reflects the thermoresponsive behavior of the microgels. Measurements were carried out in the range 20-50°C for PNIPAM and 20-55°C for PNIPMAM. As the temperature increases and the solvent becomes increasingly poor, the electrophoretic mobility increases; when the particles collapse, the charge density increases and the electrophoretic mobility increases with it. Well above the VPTT, the electrophoretic mobility no longer increases, as the size and thereby the charge density remains constant.

### 4.1.3 Interaction potential

The temperature dependence of microgel size and charge density was investigated by DLS and electrophoretic mobility (section 4.1.2.2 and section 4.1.2.5 respectively). In addition, the temperature dependent interaction potential of LE2 was studied by CLSM. At 20°C, both in the absence and presence of salt (0.1 M KCl), no sign of aggregation was observed. However, when increasing the temperature to above the VPTT (50°C) and in the presence of salt, the microgels were observed to aggregate and form volume-spanning fractal networks (Figure 4.8). In the absence of salt the formation of aggregate structures was not observed. Upon decreasing the temperature to below the VPTT, the aggregates previously present in the salty suspension were dissociated. The experiment shows that the microgels' interaction potential can be controlled by using temperature as an external stimulus (Figure 4.9). It also demonstrates that the mechanism of stabilization is different in different temperature regimes. The presence of salt, which screens electrostatic interactions, did not induce formation of aggregates below the VPTT, thus indicating that the stabilization is not solely due to electrostatics but steric stabilization dominates. Above the VPTT, the addition of salt however did induce aggregation, thus showing that the stabilization is now mainly electrostatic.

### 4.1.4 Microgel-microgel cross-linking

Microgels were functionalized with allylamine groups to enable their subsequent inter-cross-linking using glutaraldehyde as cross-linker. Glutaraldehyde carries two sites that are susceptible to nucleophilic attack by nucleophiles such as amines. In our case, this allows glutaraldehyde to bridge between amine groups on adjacent microgels, thereby forming covalent inter-microgel cross-links (Figure 4.10). It is important to note that glutaraldehyde can also bridge amine groups within the same microgel particle, thus forming intra-particle cross-links.

In order to investigate whether or not the synthesized microgels could be cross-linked, bulk

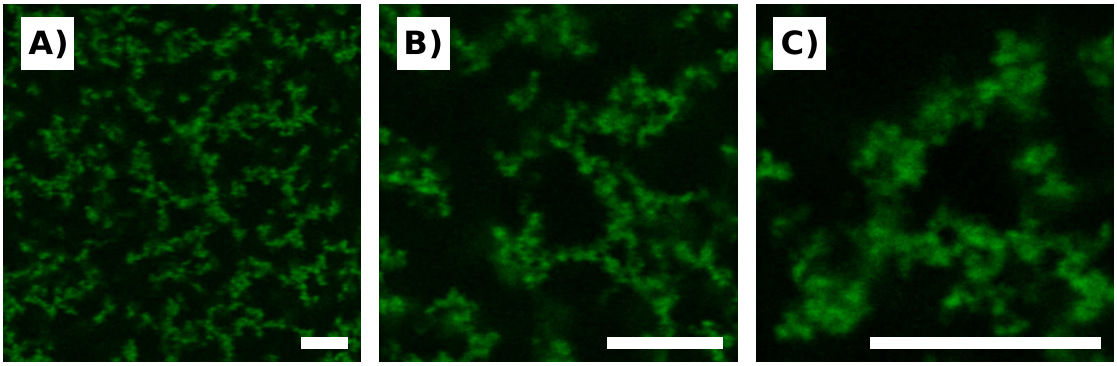


Figure 4.8: Above the VPTT and in the presence of salt (0.1 M KCl), LE2 microgels aggregate and form volume-spanning fractal networks. Scale bars are 10 $\mu$m. In the absence of salt, no aggregation takes place (not shown).

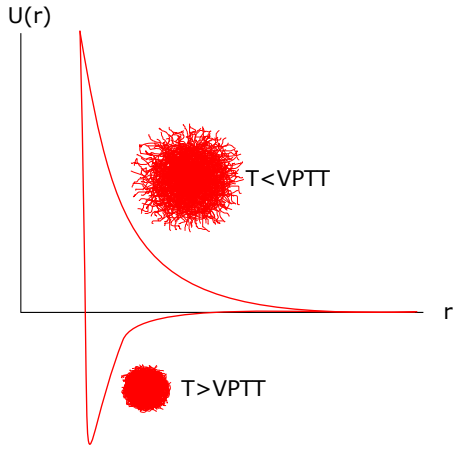


Figure 4.9: Temperature dependent interaction potential of a microgel particle.

cross-linking tests were performed. Microgel suspensions were first concentrated in Eppendorf tubes by centrifugation and removal of the supernatants. Cross-linker was then added on top of the pellets, and was allowed to diffuse into the dense suspensions. Samples were left for a minimum of four days to allow for complete cross-linking. The contents of the Eppendorf tubes were then transferred to water to check if remaining intact (Figure 4.11 A). If not intact, it would imply that cross-linking did not take place and individual microgels would diffuse apart. The pellets were left in water for a period of at least one week to properly show that the microgels were inter-cross-linked. None of the pellets showed signs of dissolution, thus proving that they are in fact cross-linked. The formed macrogels were subsequently heated to above the VPTT of the individual microgels (50°C), in order to demonstrate the thermoresponsive behavior on a macroscopic scale (Figure 4.11 B). Since the individual microgels collapse above the VPTT, and because they are cross-linked, the macrogels are expected to shrink. When allowed to cool back to room temperature, the microgels reswelled and the macrogels retained their original size.

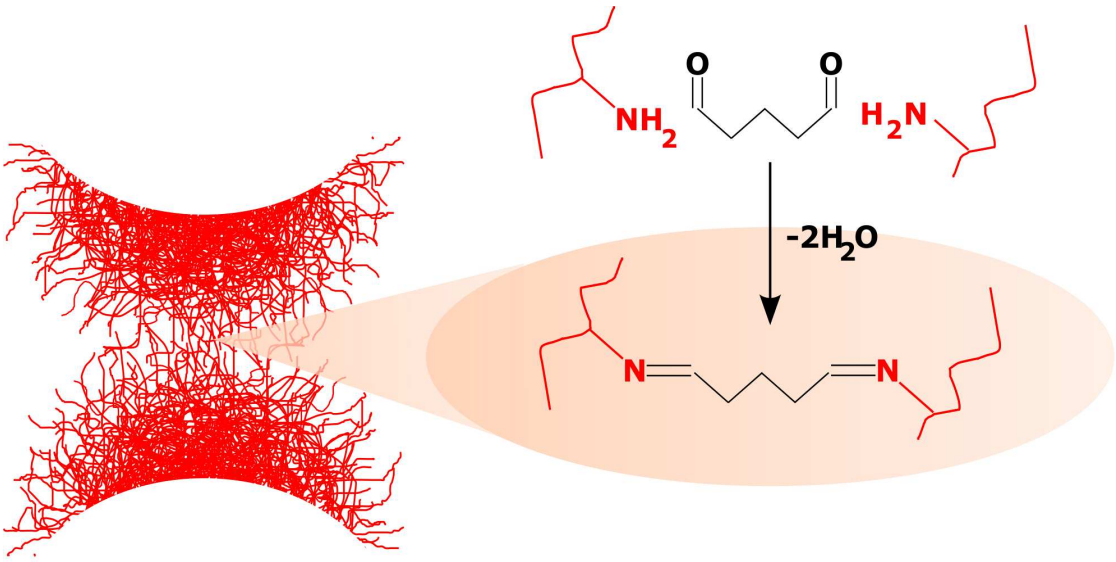


Figure 4.10: Glutaraldehyde can act as a covalent cross-linker between two adjacent microgels through reaction with amine groups on the microgels' surface.

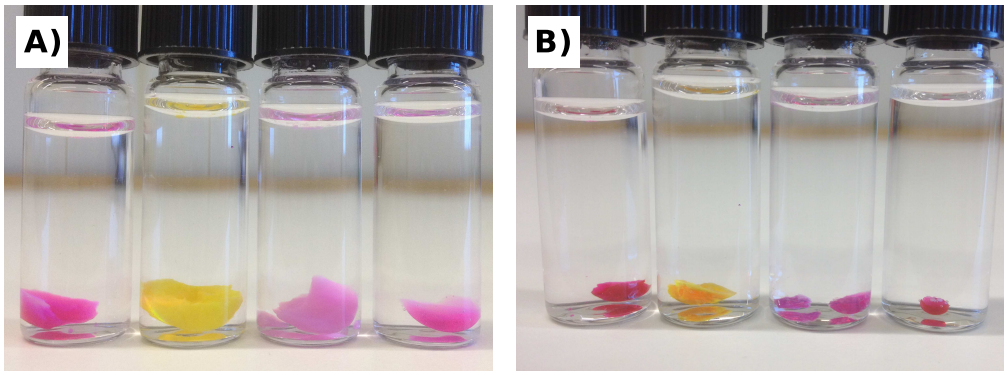


Figure 4.11: A) Cross-linked (from left to right) LE1, LE2, LE7 and LE9 macrogels remain intact when transferred into water (at room temperature). B) When increasing the temperature to 50°C (above the VPTT), the macrogels shrink. The macrogels reswell when cooled back to room temperature (not shown).

### 4.1.5 Cross-linking of microgel fractals

In order for microgel-microgel cross-linking to take place, microgels need to be in close proximity. The perhaps most obvious means of bringing microgels together is through concentration of the suspension (Section 4.1.4). Alternatively, above the VPTT and in the presence of salt, microgels are attractive and come together in large volume-spanning fractal networks (Section 4.1.3). The latter was explored in order to form macrogels, where the formed fractals where cross-linked in the presence of glutaraldehyde. Here, a suspension of LE2 (3.6 wt%), in the presence of salt and cross-linker, was heated to 50°C (above the VPPT) for three days. A control sample containing just LE2 was subject to the same treatment. When taken out of the heating chamber, the control sample was still liquid. In contrary, the salty suspension did not flow (Figure 4.12 A),

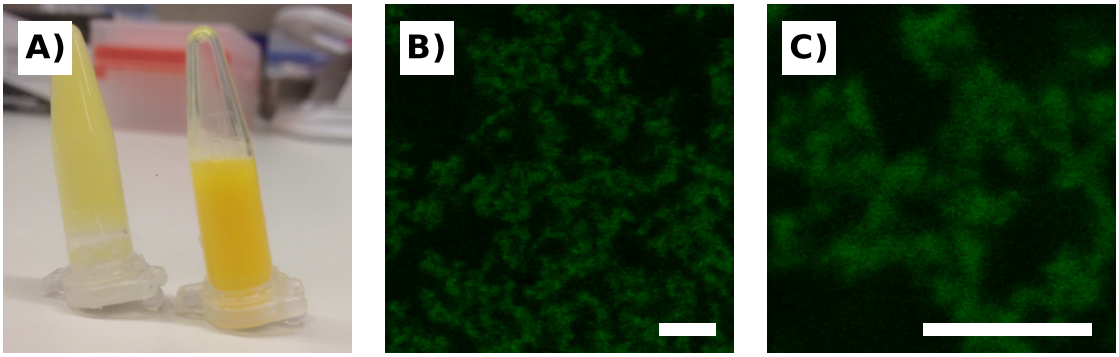


Figure 4.12: A) LE2 microgel suspensions in the presence (left) and absence (right) of salt and glutaraldehyde, respectively. Suspensions have been stored at 50°C (above VPTT) for three days. B and C) Fluorescence CLSM micrographs of the salty sample following cooling to 20°C. Scale bars are 5 $\mu$m.

thus pointing to gel formation. The suspension remained a gel when cooled to 20°C, and CLSM furthermore confirmed the presence of cross-liked fractals (Figure 4.12 B and C).

## 4.2 Microfluidics

Up to this point, amine-functionalized microgels had been synthesized and confirmed to inter-particle cross-link with glutaraldehyde. Subsequently, the microgels were used in an attempt to form colloidal molecules through microgel clustering in droplet-based microfluidics. The microfluidics cluster formation strategy involves production of microgel-containing water droplets that are subsequently shrunken to yield microgel clusters.

### 4.2.1 Microfluidics device

The microfluidics device used to form water-in-oil droplets had one inlet for the oil phase, one inlet for the dilute aqueous microgel suspension, two outlets, a junction with a diameter of 10 $\mu$m and permeable walls that allow water to diffuse out and droplets to shrink (Figure 4.13). Droplets with a diameter roughly equal to that of the fluid junction was produced in the microfluidics device (Figure 4.14). The droplets shrink as the water diffuses out through the permeable channel walls which is a requirement for the assembly of the microgel particles. Droplets imaged at the output were fluorescent and thus contain microgels, but the number of microgel particles in each droplet could not be determined because of the low resolution of the microscope. The concentration of the microgel suspensions used was chosen so that the probability maximum, according to the Poisson-distribution, for the number of particles in each droplet is four microgel particles per droplet. The concentration used might need to be further optimized once the number of particles in the droplets has been determined. Droplets have been collected from the output, but could not be successfully extracted from the oil phase. The oil itself is extremely dilute with respect to the droplets, and thus the microgel particles (clusters) in the oil can not be properly imaged without first being extracted and concentrated. However, the water droplets can not immediately be extracted from the oil but the cross-linking has to complete. If not, no covalent bonds hold the microgel clusters together and individual microgels will diffuse apart once redispersed in water.

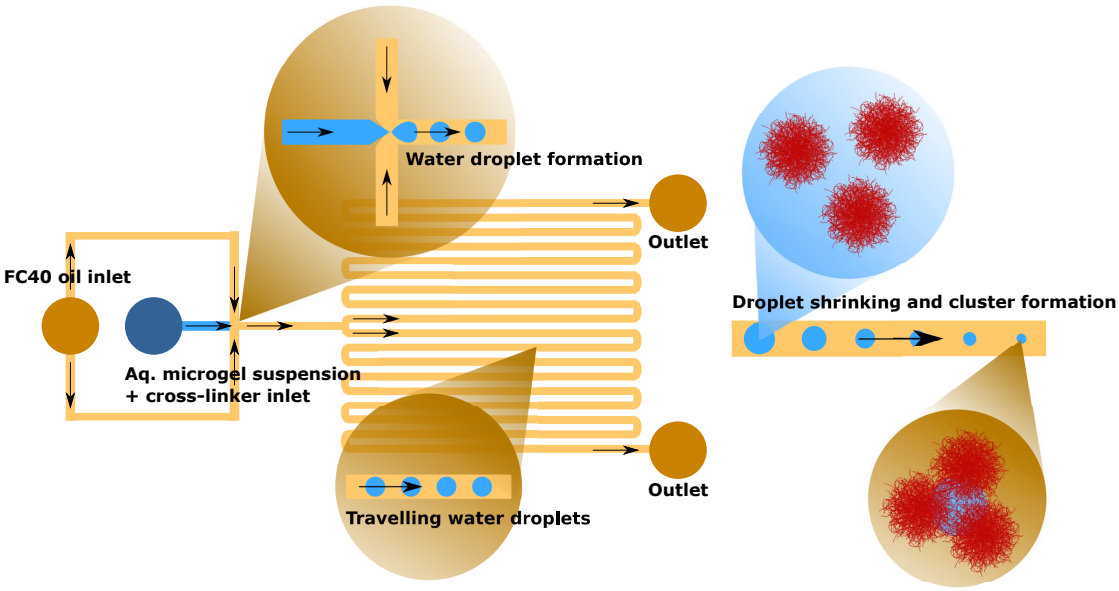


Figure 4.13: Schematic drawing of the microfluidics device.

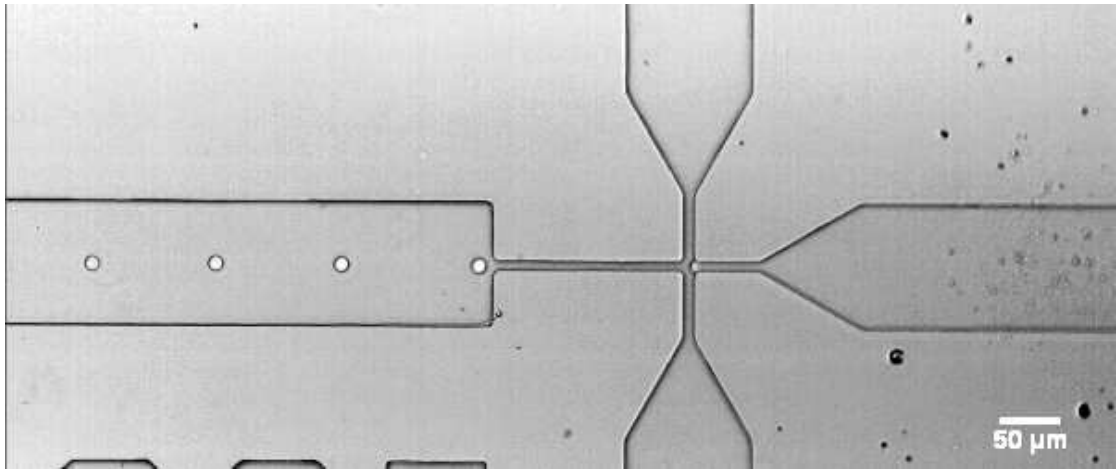


Figure 4.14: Water droplet formation in the microfluidics device, in the oil-water junction.

### 4.2.2 Microgel cluster formation

As previously mentioned, the strategy of obtaining colloidal molecules involves assisted assembly of cross-linkable microgels in droplet-based microfluidics. Microgel suspensions were mixed with glutaraldehyde prior to injection into the microfluidics device. The water droplets formed in the device thus contain a number of microgel particles as well as glutaraldehyde cross-linker. When the droplets shrink due to water diffusion, the microgels are forced closer to each other, eventually assembling into colloidal molecule-like clusters when the droplets are sufficiently small (Figure 4.13). When the particles are close to one another, glutaraldehyde can react with amine groups on the surface of adjacent microgels, thereby forming covalent microgel-microgel cross-

links that hold the clusters together. Without the cross-links present the formed clusters will only be temporary constructs held together by the interfacial tension between the water and oil. In that case the clusters will dissociate as soon as being transferred to a water solution. Furthermore, the time of cluster formation have to be fast enough so that the cross-linker is not consumed in intra-particle cross-linking before clusters are formed and inter-crosslinking can take place. The presence of microgel clusters in water solutions obtained after extraction has not yet been confirmed, but the method of extraction needs to be further optimized. Extraction of microgel clusters was carried out by adding water to the oil followed by short centrifugation. Pico break surfactant was then added and the sample was centrifuged for a short time before the water-phase, which should have contained the clusters, was collected. Alternatively, the absence of clusters may be related to inefficient droplet shrinking and cluster formation; only microgels in close proximity will be cross-linked. The rate of droplet shrinking might thus need to be optimized with respect to the rate of cross-link formation.

# Chapter 5

# Summary and Outlook

This project features the first steps toward a novel approach for obtaining thermoresponsive colloidal molecules, where amine-functionalized, cross-linkable microgels are employed in droplet-based microfluidics with the goal of forming colloidal molecule-like microgel clusters.

Four microgel systems, based on either poly(*N*-isopropylacrylamide) (PNIPAM) or poly(*N*-isopropylmethacrylamide) (PNIPMAM) and with allylamine as co-monomer, were synthesized and characterized by dynamic and static light scattering (DLS and SLS), confocal laser scanning microscopy (CLSM) and electrophoretic mobility. The microgels obtained had a hydrodynamic radius ranging from 150 to 300 nm at 20°C and was confirmed to be positively charged by electrophoretic mobility measurements. Furthermore, they were shown to possess thermoresponsive behavior in terms of size, charge density and interaction potential, as determined by DLS, electrophoretic mobility and CLSM, respectively. Concentrated microgel suspensions formed macrogels upon addition of glutaraldehyde, thus confirming the ability of the microgels to take part in microgel-microgel cross-linking. However, cross-linking does not exclusively take place between different microgels, but also internal cross-links are formed. How this alters microgel thermoresponsiveness will be subject for later studies.

Obtained microgels were used in droplet-based microfluidics where microgel-containing water droplets were produced and were allowed to shrink in order for the microgels to form clusters. However, following the microfluidics process, clusters were not successfully extracted. In this respect, the microfluidics procedure still requires more optimization before colloidal molecules can be obtained. In addition, the number of microgels in the clusters are expected to follow a statistical Poisson-distribution, which requires the development of a method that allows for separation of clusters of different sizes [17].

As a direct extension of the project, microgel clusters with two different types of microgels, one PNIPAM and one PNIPMAM, will be synthesized. This will give colloidal molecules with two different types of interaction sites, both thermoresponsive but with different thermoresponsive behavior due to different VPTTs. Furthermore, the synthesized microgels may find possible applications not related to this project, taking advantage of their cross-linking ability and thermoresponsiveness. Firstly and which has been demonstrated by Hu and Huang, colloidal crystals can be obtained [18]. Other applications include the formation of colloidal gels through the cross-linking of fractal networks above the VPTT in the presence of salt (Figure 5.1 A). Such experiments have already been initiated 4.1.5. Taking advantage of the surface activity of microgels [19, 20, 21, 22] membranes and colloidosomes can furthermore be produced (Figure 5.1 B and C). A similar approach for colloidosome formation was employed by Shah *et al.* where droplets generated by microfluidics where used as templates [9]. Finally, flower-like

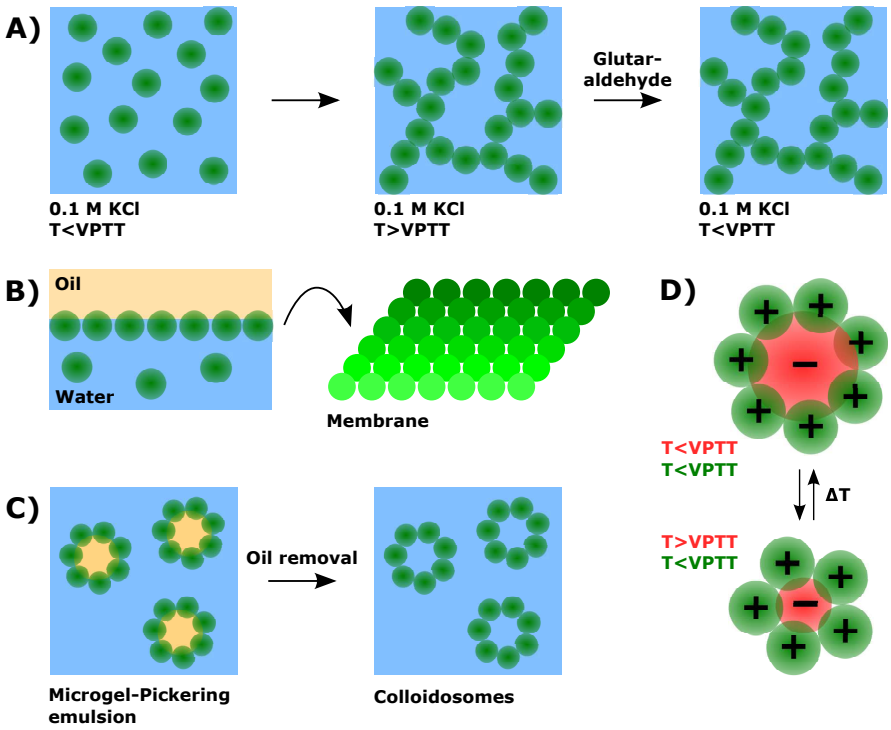


Figure 5.1: Potential future applications of cross-linkable microgels include the formation of A) colloidal gels through the formation of volume-spanning fractal networks above the VPPT of the microgels, B) membranes that can be harvested from oil-water interfaces, C) colloidosomes using emulsions as templates, and D) colloidal molecule-like clusters from microgels of opposite charge.

colloidal molecules can be produced by clustering of particles of opposite charge (Figure 5.1 D). By choosing the particles so that the core and shell particles have different VPTT, the valency (i.e. the core-to-shell particle ratio) of the assemblies can be controlled.

# Acknowledgments

I would like to thank Prof. Peter Schurtenberger for the opportunity to do this project in his group. I would also like to thank Feifei Peng and Linda Månsson for the help with the project and the thesis. I extend my gratitude to Marc for helping with light scattering measurements and Thiago and Luigi for keeping me entertained. Finally, I would like to thank Helena, Maria and Christopher for helping me get started and anyone else that made my stay at the department a pleasant experience.

# Bibliography


[1] A. van Blaaderen. Colloidal Molecules and Beyond. *Science*, 470:470–471, 2003.

[2] Y. Wang, Y. Wang, D. R. Breed, V. N. Manoharan, L. Feng, A. D. Hollingsworth, M. Weck, and D. J. Pine. Colloids with Valence and Specific Directional Bonding. *Nature*, 491:51–56, 2012.

[3] S. Saccana, W. T. M. Irvine, P. M. Chaikin, and D. J. Pine. Lock and Key Colloids. *Nature*, 464:575–578, 2010.

[4] Y. Xia, Y. Yin, Y. Lu, and J. McLellan. Template-Assisted Self-Assembly of Spherical Colloids into Complex and Controllable Structures. *Adv. Funct. Mater.*, 13:907–918, 2003.

[5] D. J. Kraft, W. Vlug, C. van Kats, A. van Blaaderen, A. Imhof, and W. Kegel. Self-Assembly of Colloids with Liquid Protrusions. *J. Am. Chem. Soc.*, 131:1182–1186, 2009.

[6] V. N. Manoharan, M. T. Elsesser, and D. J. Pine. Dense Packing and Symmetry in Small Clusters of Microspheres. *Science*, 301:483–487, 2003.

[7] S.-H. Kim, G.-R Yi, K. H. Kim, and S.-M Yang. Photocurable Pickering Emulsion for Colloidal Particles with Structural Complexity. *Langmuir*, 24:2365–2371, 2008.

[8] G. Huang, J. Gao, Z. Hu, J. V. St. John, B. C. Ponder, and D. Moro. Controlled Drug Release from Hydrogel Nanoparticle Networks. *J. Control. Release*, 94:303–311, 2004.

[9] R. K. Shah, J.-W. Kim, and D. A. Weitz. Monodisperse Stimuli-Responsive Colloidosomes by Self-Assembly of Microgels in Droplets. *Langmuir*, 26:1561–1565, 2010.

[10] C. James, A. L. Johnson, and A. T. A. Jenkins. Antimicrobial surface grafted thermally responsive pnipam-co-ala nano-gels. *Chem. Commun.*, 47:12777–12779, 2011.

[11] D. H. Everett. *Basic Principles of Colloidal Science*. The Royal Society of Chemistry, London, England, 1988.

[12] G. Fritz, V. Schädler, N. Willenbacher, and N. J. Wagner. Electrostatic Stabilization of Colloidal Dispersions. *Langmuir*, 18:6381–6390, 2002.

[13] R. Pelton. Temperature-Sensitive Aqueous Microgels. *Adv. Colloid Interface Sci.*, 85:1–33, 2000.

[14] R. Pelton and P. Chibante. Preparation of Aqueous Latices with N-Isopropylacrylamid. *Colloids and Surfaces*, 20:247–256, 1986.

[15] F. Evans and H. Wennerström. *The Colloidal Domain: Where Physics, Chemistry, Biology, and Technology Meet*. VHC Inc., New York, USA, 1994.

[16] I.-D. Block and F. Scheffold. Modulated 3d Cross-Correlation Light Scattering: Improving Turbid Sample Characterization. *Rev. Sci. Instrum.*, 81:123107(1)–123107(7), 2010.

[17] unpublished results. F. Peng.

[18] G. Huang and Z. Hu. Phase Behavior and Stabilization of Microgel Arrays. *Macromol*, 40:3749–3756, 2007.

[19] T. Ngai, S. H. Behrens, and H. Auweter. Novel Emulsions Stabilized by pH and T]emperature Sensitive Microgels. *Chem. Commun.*, 3:331–333, 2005.

[20] T. Ngai, S. H. Behrens, and H. Auweter. Environmental Responsiveness of Microgel Particles and Particle-Stabilized Emulsions. *Macromol.*, 39:8171–8177, 2006.

[21] S. Tsuji and H. Kawaguchi. Thermosensitive Pickering Emulsion Stabilized by Poly(N-isopropylacrylamide)-Carrying Particles. *Langmuir*, 24:3300–3305, 2008.

[22] B. A. Rosen B. Brugger and W. Richtering. Microgels as Stimuli-Responsive Stabilizers for Emulsions. *Langmuir*, 24:12202–12208, 2008.